Synthesis, electrochemistry and single-molecule conductance of bi-metallic 2,3,5,6-tetra(pyridine-2-yl)pyrazine based complexes

Ross Davidson,[a] Jing-Hong Liang,[b,c] David Costa Milan,[b] Bing-Wei Mao,[c] Richard J. Nichols,[b] Simon J. Higgins,[b] Dmitry S. Yufit,[a] Andrew Beeby,[a] Paul J. Low[d]*.

a) Department of Chemistry, Durham University, South Rd, Durham, DH1 3LE, UK

b) Department of Chemistry, University of Liverpool, Crown St, Liverpool, L69 7ZD, UK

c) State Key Laboratory of Physical Chemistry of Solid Surfaces and College of Chemistry and Chemical Engineering, Xiamen University, Xiamen 361005, Fujian, China.

d) School of Chemistry and Biochemistry, University of Western Australia, Stirling Highway, Perth, WA 6009, Australia

KEYWORDS

bis(terpyridyl), molecular electronics, metal complexes, single molecule conductance

ABSTRACT: The ligands 4-((methyl)sulfane)phenyl)-2,2′:6′,2″-terpyridine (**L**^{1}) , 4-((4'-(methyl)sulfane)phenylethynyl)-2,2′:6′,2″-terpyridine (**L**^{2}) and bis(tridentate) bridging ligand 2,3,5,6-tetra(pyridine-2-yl)pyrazine (tpp) have been used to prepare the complexes [Ru(**L**^{1})$_2$][PF$_6$]$_2$ ([**1**][PF$_6$]$_2$, [Ru(**L**^{2})$_2$][PF$_6$]$_2$ ([**2**][PF$_6$]$_2$), [{(**L**^{1})Ru}(μ-tpp){Ru(**L**^{1})}][PF$_6$]$_4$ ([**3**][PF$_6$]$_4$) and [{(**L**^{2})Ru}(μ-tpp){Ru(**L**^{2})}][PF$_6$]$_4$ ([**4**][PF$_6$]$_4$). Crystallographically determined structures give S…S distances of up to 32.0 Å in [**4**]$^{4+}$. On the basis of electrochemical estimates, the HOMOs of these complexes fall between −5.55 and −5.85 eV, close to the work function of clean gold (5.1 - 5.3 eV). The decay of conductance with molecular length across this series of molecules is approximately exponentially, giving rise to a decay constant (pseudo β-value) of 1.5 nm^{-1}, falling between decay factors oligoynes and oligophenylenes. The results are consistent with a tunnelling mechanism for the single molecule conductance behavior.

INTRODUCTION

With the increased availability of STM and break-junction technology great strides have been made in the understanding of single molecule conductance,[1] particularly with regards to pure organic compounds such as polyynes,[2, 3] oligophenylenes,[4] and oligoaryleneethynylenes.[5] More recently, attention has been turned to the role that metal centers and complexes may play when incorporated into the backbone of a wire-like molecule.[6-10] These metal complexes are of a special interest in the realm of molecular electronics, as they hold the potential for finer tuning of the molecular orbitals to match the Fermi levels of the electrodes, and also the possibilities to augment electronic characteristics through accessing available redox levels,[11] electrochemical gating,[12, 13] redox or optical switching,[14] and magnetic effects,[15] as well as high thermoelectric efficiency.[16]

Metal complexes based on 2,2′:6′,2″-terpyridine (tpy) ligands have proven to be valuable for evaluation of many of these features of metal complexes in molecular electronics, and to-date these are some of the most studied metal complexes to be incorporated into a metal|molecule|metal junction and related molecule|metal assemblies.[11, 12, 17-25] The $\{M(tpy)_2\}^{n+}$ structural element has proven particularly popular being easily accessed synthetically and functionalised to give linear molecular geometries,[26] featuring a wide range of metal ions, allowing a selection of physical and chemical properties relating the charge, size, redox and magnetic properties of the complex to be readily examined. The 2,3,5,6-tetra(pyridine-2-yl)pyrazine (tpp) ligand, which may be regarded as a 'back-to-back' fused bis-tpy ligand, is a valuable structural element when seeking to figuratively and literally extend these studies. The tpp ligand, used in conjugation with tpy co-ligands, provides a convenient entry point to linear, multi-metallic assemblies in which the metal centres can be strongly coupled,[27-31] and is well-suited to use in the construction of molecular arrays both in solution and from 'on-surface' coordination chemistry approaches.[20, 21]

We now report the synthesis, electrochemical and single molecule conductance behaviour of mono and bimetallic ruthenium complexes based on $[Ru(tpy)_2]^{2+}$ and $[\{(tpy)Ru\}(\mu\text{-}tpp)\{Ru(tpy)\}]^{4+}$ structural motifs. The multi-metallic complexes are shown to be capable of serving as wire-like assemblies of up to 3 nm long.

EXPERIMENTAL SECTION

General details. Microwave reactions were performed in a Biotage Microwave Synthesizer (Model Initiator 2.5). NMR spectra were recorded in deuterated solvent solutions on Bruker DRX-400 and Varian Inova 300, 400, 500 spectrometers and referenced against solvent resonances (^{1}H, ^{13}C). Electrospray mass spectra (ESMS) were recorded on a TQD mass spectrometer (Waters Ltd, UK) in acetonitrile. Atmospheric Solids Analysis Probe mass spectra (ASAP-MS) were collected on a LCT Premier XE mass spectrometer (Waters Ltd, UK) in dichloromethane. Microanalyses were performed by Elemental Analysis Service, London Metropolitan University, UK. Electrochemical analyses of the complexes were carried out using a PalmSens EmStat^{2} potentiometer, with platinum working, platinum counter and platinum pseudo reference electrodes, from solutions in acetonitrile containing 0.1 M supporting electrolyte (tetrabutylammonium hexafluorophospate, NBu_4PF_6), scan rate = 100 mV s^{-1}. The ferrocene/ferrocinium couple was used as the internal reference.

Analytical grades of solvents were used. The compounds 4′-(((trifluoromethyl)sulfonyl)oxy)-2,2′:6′,2″-terpyridine (tpyOTf)[32], (4-ethynylphenyl)(methyl)sulfane ($MeSC_6H_4C{\equiv}CH$),[33] 4-((methyl)sulfane)phenyl)-2,2′:6′,2″-terpyridine (**L**^{1}),[34] $[Ru(\mathbf{L}^{1})_2][PF_6]_2$ ($[\mathbf{1}][PF_6]_2$)[34] and $\{Cl_3Ru\}(\mu\text{-tpp})\{RuCl_3\}$[35] were synthesised according to literature methods. All other chemicals were sourced from standard suppliers. Hydrated ruthenium chloride, $RuCl_3{\cdot}nH_2O$ was assumed to be of approximate composition $RuCl_3{\cdot}3H_2O$.

Synthesis.

4′-((4-(methylthio)phenyl)ethynyl)-2,2′:6′,2″-terpyridine (**L**^{2}). Triethylamine (NEt_3, 7 mL) was added to a solution containing tpyOTf (250 mg, 0.65 mmol) and $MeSC_6H_4C{\equiv}CH$ (96 mg, 0.65 mmol) in THF (20 mL). The solution was freeze-pump-thawed three times before $Pd(PPh_3)_4$ (75 mg, 0.065 mmol) was added. The solution was refluxed overnight in the dark after which time the solvent was removed. The solid residue was extracted in dichloromethane and filtered. The filtrate was passed down a silica column initially with neat CH_2Cl_2 then CH_2Cl_2:acetonitrile (1:1) to elute the product. The main fraction was collected, dried and washed with methanol to remove the remaining impurities, giving a white solid. Crystals were grown via the slow evaporation of a hexane/dichloromethane solution. Yield: 193 mg (78%). ASAP-MS: 380 m/z $[MH]^+$. ^{1}H NMR ($CDCl_3$): δ 8.70 (d (J^1_{HH} = 5 Hz), 2H), 8.60 (d (7), 2H), 8.53 (s, 2H), 7.85 (t (7), 2H), 7.44 (d (7), 2H), 7.33 (t (7), 2H), 7.20 (d (7), 2H), 2.48 (s, 3H) ppm. ^{13}C{^{1}H} NMR ($CDCl_3$): δ. 155.5, 155.3, 149.3, 140.5, 137.0, 133.5, 132.1, 125.7, 124.0, 122.7, 121.2, 118.5, 93.8, 87.5, 15.2 ppm. Anal. Calc. for $C_{24}H_{17}N_3S$: C, 75.96; H, 4.52; N, 11.07 %. Found: C, 75.86; H, 4.45; N, 11.02 %.

*[Ru(**L**^{2})$_2$][PF$_6$]$_2$* [**2**][PF_6]$_2$. The ligand **L**^{2} (100 mg, 0.26 mmol) and $RuCl_3{\cdot}3H_2O$ (34 mg, 0.13 mmol) were added to ethylene glycol (4 mL). The resulting suspension was degassed by bubbling nitrogen through it before being heated by microwave to 160°C for 30 minutes. The red solution was poured into an aqueous, saturated KPF_6 solution forming a red precipitate. The precipitate was collected by filtration and washed thoroughly with water and air dried. The red solid was exracted in acetone, filtered and the filtrate taken to dryness, leaving a red residue. This residue was disolved in the minimum volume of CH_2Cl_2 and purified by elution through a

neutral alumina column with an acetonitrile: CH_2Cl_2 (1:1). The orange band was collected and the solvent removed leaving the title product. Crystals were grown by vapour diffusion of diethyl ether into an acetonitrile solution. Yield: 119 mg (80 %). ESMS: 430 m/z $[M]^{2+}$. ^{1}H NMR($CDCl_3$): δ 8.87 (s, 4H), 8.52 (d (J^1_{HH} = 8 Hz), 4H), 7.96 (t (8), 4H), 7.71 (d (8), 4H), 7.44-7.42 (m, 8H), 7.20 (t (7), 4H), 2.59 (s, 6H) ppm. $^{13}C\{^1H\}$ NMR ($CDCl_3$): δ. 157.5, 155.1, 152.6, 142.6, 138.2, 132.4, 130.5, 127.6, 125.7, 125.1, 124.5, 117.0, 97.11, 86.3, 14.0 ppm. Anal. Calc. for $C_{48}H_{34}F_{12}N_6P_2RuS_2$: C, 50.13; H, 2.98; N, 7.31 %. Found: C, 50.00; H, 3.00; N, 7.31 %.

*[{(**L**^{1})Ru}(μ-tpp){Ru(**L**^{1})}][PF$_6$]$_4$* [**3**][PF_6]$_4$. The compounds **L**^{1} (128 mg, 0.36 mmol) and {Cl_3Ru}(μ-tpp){$RuCl_3$} (100 mg, 0.12 mmol) were added to ethylene glycol (4 mL). This suspension was degassed by bubbling nitrogen through it before being heated by microwave to 160°C for 30 minutes. The purple solution was poured into an aqueous saturated KPF_6 solution forming a purple precipitate. The precipitate was collected by filtration and washed thoroughly with water and air dried. The purple solid was washed off the frit with acetone, and the filtrate collected and solvent removed, leaving a purple residue. This was eluted down a neutral alumina column with acetonitrile:CH_2Cl_2 (1:1) collecting the purple band; the solvent was removed leaving the title product. Crystals were grown by vapour diffusion of diethyl ether into an acetonitrile solution. Yield: 97 mg (43 %). ESMS: 325 m/z $[M]^{4+}$. ^{1}H NMR($CDCl_3$): δ 9.15 (s, 4H), 8.99 (d (J^1_{HH} = 8 Hz), 4H), 8.79 (d (8), 4H), 8.26 (d (8), 4H), 8.10 (t (7), 4H), 7.95 (t (8), 4H), 7.85 (d (6), 4H), 7.76 (d (6), 4H), 7.70 (d (7), 4H), 7.45 (t (7), 4H), 7.32 (t (7), 4H), 2.70 (s, 6H) ppm. $^{13}C\{^1H\}$ NMR ($CDCl_3$): δ. 157.8, 155.0, 154.7, 154.0, 153.1, 149.8, 149.3, 143.3, 139.0, 137.8, 132.3, 129.4, 129.2, 128.2, 127.6, 126.4, 125.0, 121.7, 14.2 ppm. Anal. Calc. for $C_{68}H_{50}F_{24}N_{12}P_4Ru_2S_2$: C, 43.41; H, 2.68; N, 8.93 %. Found: C, 43.50; H, 2.84; N, 8.91 %.

[{($\mathbf{L^2}$)Ru}(μ-tpp){Ru($\mathbf{L^2}$)}][PF_6]$_4$ [**4**][PF_6]$_4$. The compound was prepared using the same procedure as for described for [**3**][PF_6]$_4$ except $\mathbf{L^2}$ was used in place of $\mathbf{L^1}$. Yield: 106 mg (46 %). ESMS: 337 m/z $[M]^{4+}$. ^{1}H NMR($CDCl_3$): 9.03 (s, 4H), 9.00 (d (J^1_{HH} = 8 Hz), 4H), 8.67 (d (8), 4H), 8.11 (t (8), 4H), 7.97 (t (8), 4H), 7.83 (d (6), 4H), 7.78-7.76 (m, 8H), 7.48-7.45 (m, 8H), 7.36 (t (6), 4H), 2.62 (s, 6H) ppm. $^{13}C\{^1H\}$ NMR ($CDCl_3$): δ. 157.1, 154.8, 154.7, 154.0, 153.3, 142.9, 139.1, 137.9, 132.6, 132.5, 129.5, 129.3, 127.9, 127.4, 125.7, 125.0, 116.8, 98.1, 86.2, 14.0 ppm. Anal. Calc. for $C_{72}H_{50}F_{24}N_{12}P_4Ru_2S_2 \cdot 4H_2O$: C, 43.21; H, 2.92; N, 8.40 %. Found: C, 43.21; H, 2.57; N, 8.72 %.

Single molecule conductance measurements. Gold on glass substrates (Arrandee, Schröer, Germany) were rinsed with acetone and then flame-annealed with a butane torch until the slide glowed with a very slight orange hue. The slide was retained in this state for about 20 seconds during which time the torch was kept in motion across the sample to avoid deleterious overheating. This procedure was performed three times to generate extended Au (111) terraces, as seen by STM imaging. The freshly annealed substrates were immersed in a 10^{-4} M acetonitrile (99.9% Chromasolv Plus for HPLC) solution of the complex under investigation for 1 minute, after which time the gold sample was removed and washed with ethanol and then dried in a flow of argon. The short immersion time and low concentration of solution were chosen to promote low molecular coverage of the gold surface, which favour the formation of single molecule over multi-molecular junctions.

Conductance values of those compounds and the break off-distance were obtained with a STM (Agilent 5500 SPM microscope), using the *I*(*s*) technique.[36, 37] In this method an

electrochemically etched gold tip is approached close to the substrate surface and then retracted with the tunnelling current (*I*) recorded against distance (*s*). In the case where molecular junctions are formed, significant deviations from the usual exponential decay of current are observed, with marked current plateaus and steps appearing as the tip was retracted. The step is seen as the tip is retracted beyond the maximal stretched length of the junction, with the molecular bridge breaking, which leads to the sharp decrease in current and the observed step-like feature. The resulting *I*(*s*) curves are binned in current divisions (0.025 nS) and plotted to give a conductance histogram comprised of hundreds of scans which show plateaus synonymous with molecular junction formation.

X-ray Crystallography. The single crystal X-ray data for all compounds were collected at 120.0(2) K on a Bruker D8Venture 3-circle diffractometer (Photon100 CMOS detector, IμS microsource, focusing mirrors, λMoKα, λ = 0.71073 Å) equipped with Cryostream (Oxford Cryosystems) open-flow nitrogen cryostat. Following multi-scan absorption corrections and solution by direct methods, the structures were refined against F^2 with full-matrix least-squares using the SHELXTL[38] and OLEX2[39] software. Anisotropic displacement parameters were employed for the non-disordered non-hydrogen atoms. Disordered atoms in the structure [**2**][PF_6]$_2$ were refined isotropically with fixed SOF = 0.5 for [PF_6]$^-$ anion and 0.4:0.6 for terminal Me-group. All H-atoms were added at calculated positions and refined by use of riding models with isotropic displacement parameters based on those of the parent atom. The structures [**2**][PF_6]$_2$ and [**4**][PF_6]$_4$ alongside with well determined acetonitrile solvent molecules contain some severely disordered solvent molecules which could not be identified and refined. Their contribution to the structural factors was taken into account by applying MASK procedure of

OLEX2 program package (40 and 13 e for the structures [**2**][PF_6]$_2$ and [**4**][PF_6]$_4$ respectively). The crystallographic and refinement parameters are listed in supporting information. Crystallographic data for the structures have been deposited with the Cambridge Crystallographic Data Centre as supplementary publication CCDC-1050880-1050882.

Computational studies. All the calculations were performed with the Gaussian 09 program package,[40] using the B3LYP functional.[41, 42] A comparison was made between models using SDD basis set for all atoms or LANL2DZ basis set for Ru and 6-31G(d) for all other atoms.[43, 44] Based on agreement with the crystallographic data, the LANL2DZ/6-31G(d) basis set was chosen.

RESULTS AND DISCUSSION

Synthesis. The elementary design of compounds for single molecule conductance studies within an STM-based metal|molecule|metal junction calls for a linear or pseudo linear molecular fragment terminated by suitable surface binding groups at each end of the molecule.[37] Here, the thiomethyl (-SMe) moiety was chosen as the surface contacting or anchoring group,[45, 46] allowing for good contact to gold substrates and the STM tip and compatibility with subsequent synthetic steps, without the additional complications of the protecting group strategies involved in the use of thiolates.[47] The parent ligand, 4-((methyl)sulfane)phenyl)-2,2′:6′,2″-terpyridine (**L**$^{\mathbf{1}}$) bearing the SMe moiety was synthesised by the previously reported route involving a Kröhnke condensation of 2-acetylpyridine with 4-(methylthio)benzaldehyde (Scheme 1).[34] The new, extended ligand **L**$^{\mathbf{2}}$ was synthesised by cross-coupling of tpyOTf with the (4-

ethynylphenyl)(methyl)sulfane ($MeSC_6H_4C{\equiv}CH$) in an analogous fashion to that described for other 4-ethynyl-substituted terpyridines previously reported (Scheme 2).[48-50]

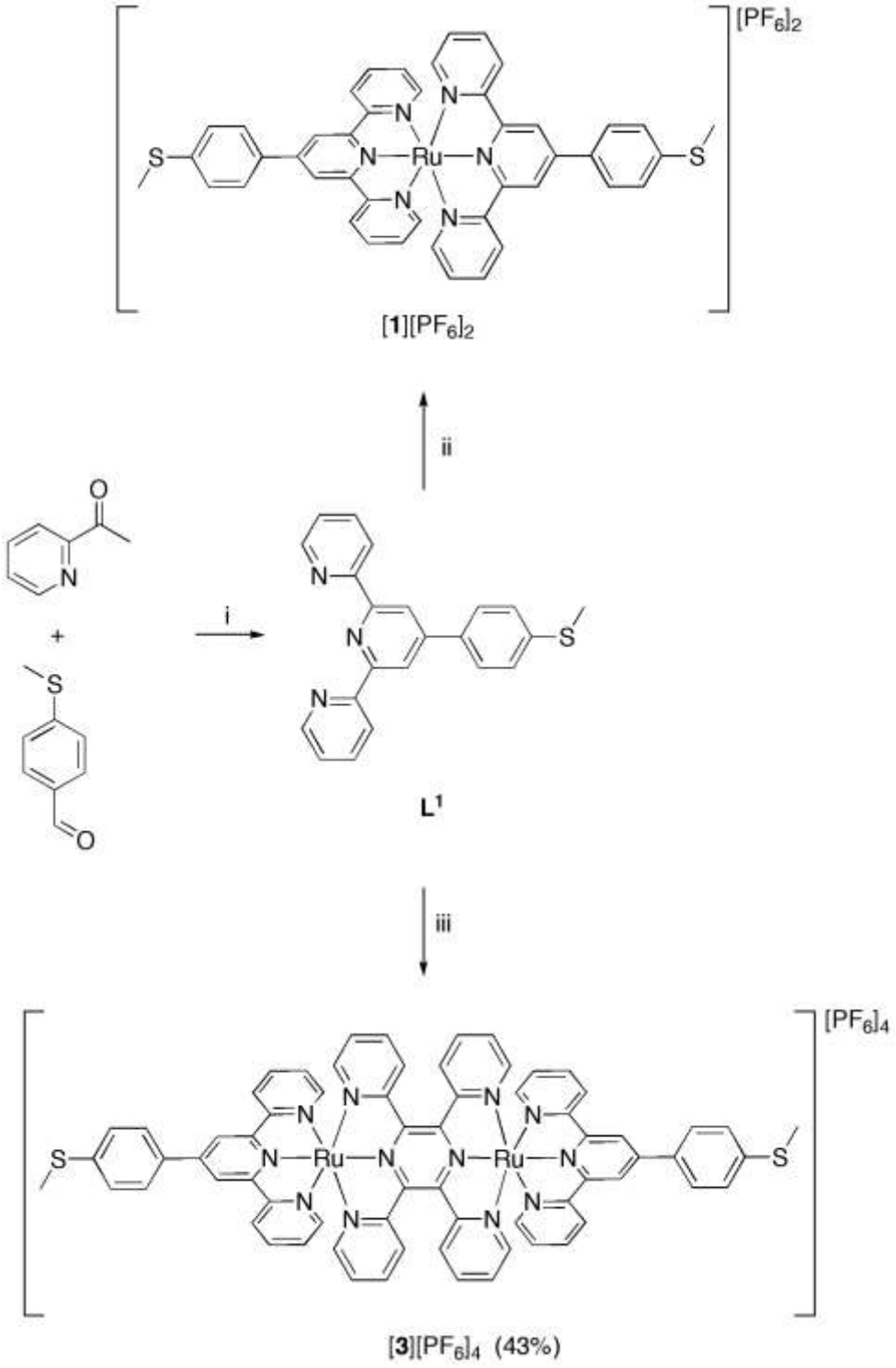

Scheme 1. Synthetic scheme for $\mathbf{L^1}$, [**1**][PF_6]$_2$ and [**3**][PF_6]$_4$. i) EtOH and NH_4Ac. ii) a) $RuCl_3 \cdot 3H_2O$, methanol, ethyl morpholine b) NH_4PF_6. iii) a) {Cl_3Ru}(μ-tpp){$RuCl_3$}, ethylene glycol, 160°C, 30 min b) KPF_6

For reference purposes, the homoleptic mono-nuclear complexes [**1**][PF_6]$_2$ and [**2**][PF_6]$_2$ were prepared from reactions of $RuCl_3 \cdot 3H_2O$ with $\mathbf{L^1}$ (Scheme 1) and $\mathbf{L}^2$ (Scheme 2), respectively. The compound [**1**][PF_6]$_2$ was prepared by the literature method as described by Constable *et al*. from the reaction of $\mathbf{L^1}$ and $RuCl_3 \cdot 3H_2O$ in refluxing methanol with a promoting amine (e.g. ethyl morpholine),[51] followed by filtration and precipitation with the addition of NH_4PF_6 (method *i*) (Scheme 1).[34] For [**2**][PF_6]$_2$ both this approach (method *i*) and an alternative procedure involving microwave heating of a suspension of $RuCl_3 \cdot 3H_2O$ and $\mathbf{L^2}$ in ethylene glycol, followed by precipitation into aqueous KPF_6 (method *ii*) were explored. In this instance both methods gave similar yields, method *ii* being favoured in this report for its greater convenience (Scheme 2).

The analogous bimetallic complexes [**3**][PF_6]$_4$ and [**4**][PF_6]$_4$ were targeted through combination of the terminal ligands $\mathbf{L^1}$ and $\mathbf{L^2}$ with the bis(tridentate) bridging ligand 2,3,5,6-tetra(pyridine-2-yl)pyrazine (tpp) (Scheme 1, Scheme 2). Reaction of $RuCl_3(\mathbf{L^1})$ [52] with tpp under either conventional or microwave heating gave only the polymeric complex of ruthenium and tpp. Similarly, conventional heating of an excess of either $\mathbf{L^1}$ or $\mathbf{L^2}$ with the bi-ruthenium trichloride complex {Cl_3Ru}(μ-tpp){$RuCl_3$}[35] also gave ruthenium-tpp polymer, presumably as a result of competing decomplexation / coordination processes. However, under microwave heating, from {Cl_3Ru}(μ-tpp){$RuCl_3$} and either $\mathbf{L^1}$ or $\mathbf{L^2}$ a mixture consisting of the desired bimetallic

products with small amounts of the homoleptic tpy complexes was formed. These bi- and mononuclear complexes were readily separated chromatographically, providing a convenient route to [**3**][PF_6]$_4$ (43 %) and [**4**][PF_6]$_4$ (46 %).

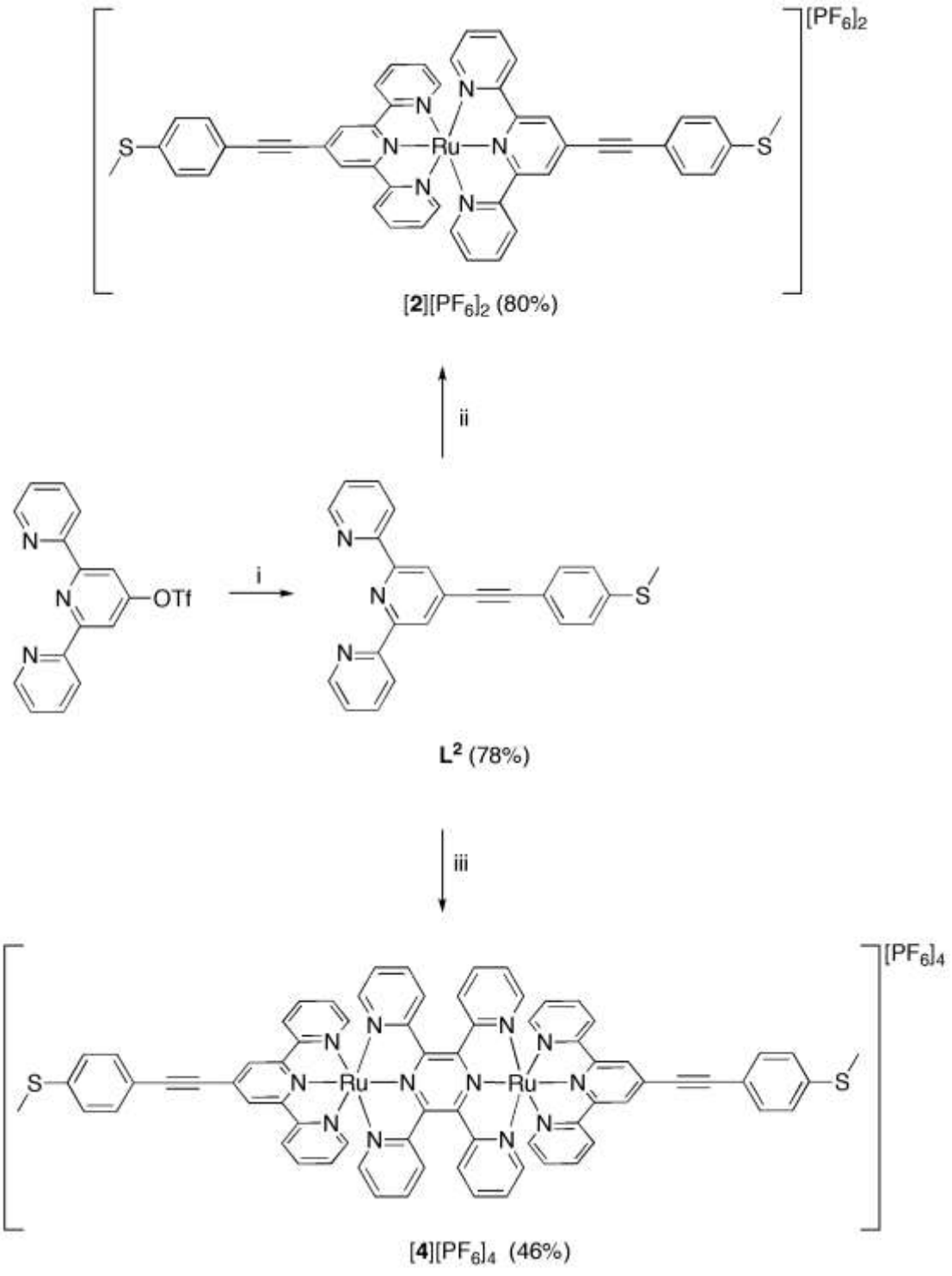

Scheme 2. Synthetic scheme for $\mathbf{L^2}$, [**2**][PF_6]$_2$ and [**4**][PF_6]$_4$. i) $MeSC_6H_4C{\equiv}CH$, $Pd(PPh_3)_4$, NEt_3 and THF. ii) a) $RuCl_3{\cdot}3H_2O$, ethylene glycol, microwave, 160°C, 30 min. b) KPF_6; iii) {Cl_3Ru}(μ-tpp){$RuCl_3$}, ethylene glycol, microwave, 160°C, 30 min. b) KPF_6.

Molecular Structures.

The structure $\mathbf{L^2}$ contains two virtually identical crystallographically independent molecules A and B (one of the molecules is shown in Figure 1), selected bond lengths and angles given in supporting information. The structure shows the (4-ethynylphenyl)(methyl)sulfane group attached to the terpyridine (tpy) motif at the 4-position, confirming the assignment by NMR spectroscopy and mass spectrometry. The three pyridine rings are almost co-planar. The nitrogen atoms on the external pyridine rings are directed toward the substituted group of the central pyridine, a common feature with tpy derivatives due largely to intramolecular hydrogen bonding. The phenylene ring (C18-C21) is rotated about the ethynyl bond relative to the tpy moiety by 21.6 ° (molecule A) and 24.3 ° (molecule B).

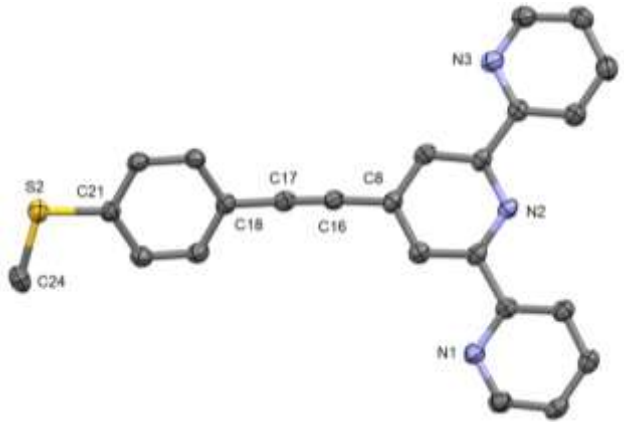

Figure 1. A plot of Molecule A in the structure $\mathbf{L^2}$, with hydrogen atoms omitted for clarity. Thermal ellispsoids are plotted at 50 %.

The cation in the structure [**2**][PF_6]$_2$·CH_3CN is shown in Figure 2, selected bond lengths and angles are given in the supporting information. The structure shows the two $\mathbf{L^2}$ ligands coordinated to the ruthenium centre via the tpy units giving an octahedral 'N_6' coordination sphere, confirming the assignment of the structure made by NMR spectroscopy and mass spectrometry. The axial Ru-N bond lengths are 1.967(3) (Ru1-N2) and 1.966(3) Å (Ru1-N5) similar to those of [Ru(tpy)$_2$][PF_6]$_2$·2CH_3CN.[53] The ethynyl-substituted phenylene groups are almost co-planar with the associated tpy fragments, although in the absence of any significant structural evidence for extensive delocalisation, the orientation of this group is likely governed by packing forces. The alkyne bond lengths show no significant difference when the structures of the free ligand and complex are compared (C16-C17 = 1.180(6) Å, [**2**]$^{2+}$; 1.204(3) Å, $\mathbf{L^2}$). Overall, this gives a S…S distance of approximately 26.5 Å in [**2**]$^{2+}$, 4.9 Å longer than that in [Ru($\mathbf{L^1}$)$_2$][PF_6]$_2$.[34]

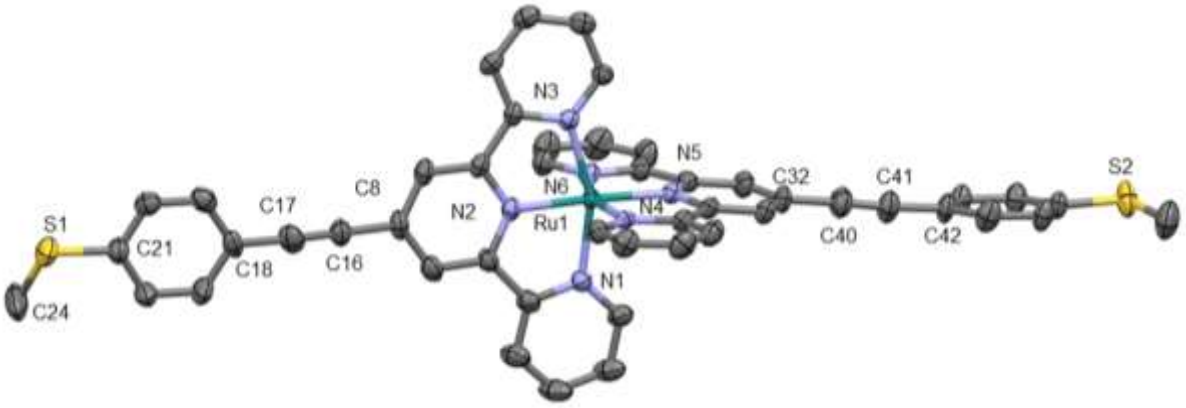

Figure 2. A plot of the cation in the crystal structure of [**2**][PF_6]$_2$·CH_3CN, with hydrogen atoms and anions have been omitted for clarity. Thermal ellispoids are plotted at 50 %.

The bimetallic cation in the structure [**4**][PF_6]$_4$·3CH_3CN is shown in Figure 3; selected bond lengths and angles are given in the supporting information. The structure shows two ruthenium atoms coordinating the phenazine ring of tpp and to its peripheral pyridines and the remaining "N6" coordination sphere of the metals was occupied via $\mathbf{L}^{\mathbf{2}}$. The tpp ligand displays the typical bending of the phenazine ring, resulting in a gracefully curved shape to the molecular tetracation. As with [**2**][PF_6]$_2$ the alkyne bond lengths remain unchanged from that of the ligand with C41-C40 = 1.198(12) and C64-C65 = 1.198(10) Å. The ruthenium-nitrogen bond lengths for [**4**][PF_6]$_4$ Ru1-N8 = 1.994(5) and Ru1-N1 = 1.975(5) Å are also similar to the comaprable distances found in [{(tpy)Ru}(μ-tpp){Ru(tpy)}][PF_6]$_4$ (1.96(2), 1.98(2) and 1.96(2), 2.00(2) Å)[54] and [**2**][PF_6]$_2$·CH_3CN,suggesting that the electronic nature of the Ru-tpp-Ru remains unaffected by the addition of the ethynyl phenyl groups. Overall, this gives an S…S distance of 32.0 Å.

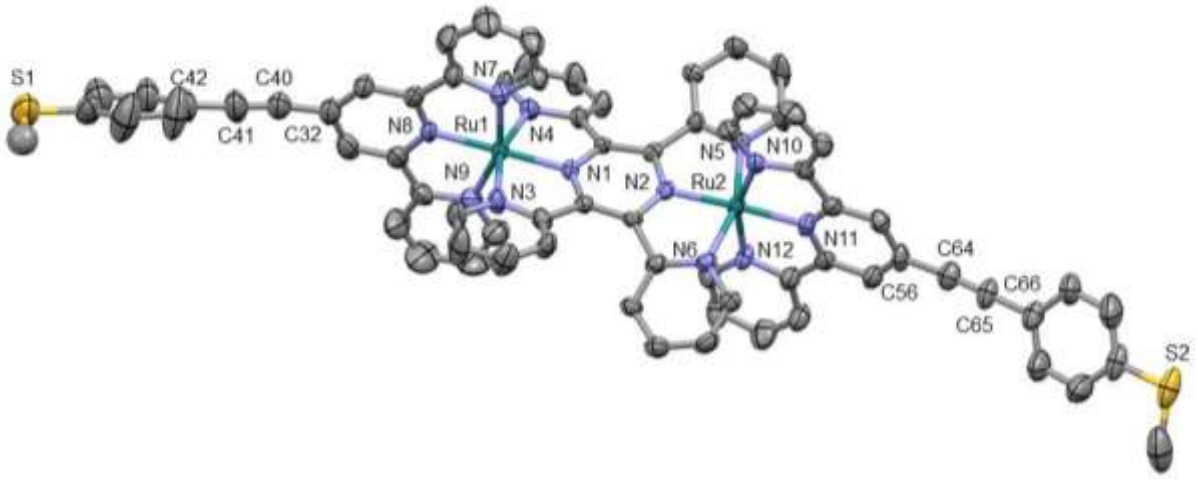

Figure 3. Cation in the crystal structure of [**4**][PF_6]$_4$·3CH_3CN, with hydrogen atoms, solvent molecules and anions removed for clarity. Thermal ellispsoids are plotted at 50%

Cyclic Voltammetry. Cyclic voltammograms were recorded for mononuclear [**2**][PF_6]$_2$ in 0.1 M $TBAPF_6$ in acetonitrile, and referenced against ferrocene (i.e. $E_{½}$ $FeCp_2$ / $[FeCp_2]^+$ = 0.00 V). The response of [**1**][PF_6]$_2$ under the same conditions having been described earlier.[34] These complexes each exhibit a single oxidation wave at 0.87 ([**1**][PF_6]$_2$) and 1.06 V ([**2**][PF_6]$_2$), assumed to be primarily metal-based (Ru(II)/Ru(III)).[51] A single broad reduction wave at −1.49 V was also observed for [**2**][PF_6]$_2$ (Table 1), presumed to be two 1e$^-$ waves (resolved for [**1**][PF_6]$_2$) overlapping. The peak-to-peak separation (ΔE_p) of the oxidation wave in [**2**][PF_6]$_2$ (93 mV) compares with that of the internal ferrocene couple (82 mV). However, the significant increase in ΔE_p associated with the reduction process (179 mV), suggests that this feature may be associated with two redox events in close succession, which is entirely consistent with the sequential reduction of the tpy ligands. A second chemically irreversible oxidation event was observed near 1.08 V for [**1**][PF_6]$_2$ and 1.22 V for [**2**][PF_6]$_2$. On the basis of irreversible

oxidations observed for $\mathbf{L}^1$ and $\mathbf{L}^2$ between 1.1 - 1.2 V these irreversible processes in the complexes can be attributed to the oxidation of the thiomethyl fragment.

The electrochemical response of bimetallic $\{L_nRu^{II}\}(\mu\text{-tpp})\{Ru^{II}L_n\}$ complexes have been studied extensively, giving rise to Robin–Day class III mixed-valence complexes, or radical cations with a non-innocent bridging phenazine ring, on one-electron oxidation.[31, 55] As with similar complexes, the voltammogram of both [**3**][PF_6]$_4$ and [**4**][PF_6]$_4$ in acetonitrile (0.1 M NBu_4PF_6) display two one-electron oxidation waves attributed to the (formally) Ru(II,II) / Ru(II,III) and Ru(II,III) / Ru(III,III) redox couples (0.76 and 1.27 V for [**3**][PF_6]$_4$, and 0.90 and 1.39 V for [**4**][PF_6]$_4$)[56] (Figure 4, Table 1), although the tpp ligand is almost certainly redox non-innocent. A third irreversible oxidation event at 1.88 V ([**3**][PF_6]$_4$) and 1.93 V ([**4**][PF_6]$_4$) is also observed and attributed to the oxidation of the thiomethyl groups. The potential for the first oxidation of [**4**][PF_6]$_4$ is 50 mV more positive than that of [**3**][PF_6]$_4$, a consequence of the presence of the electron-withdrawing alkyne moiety, as was observed for [**1**][PF_6]$_2$ and [**2**][PF_6]$_2$. An even larger shift (120 mV) is apparent when the second oxidation potentials are compared, suggesting that the redox properties are not solely localised to the Ru-tpp-Ru cores. The large separation of the two oxidation events points to the significant thermodynamic stability of the formally Ru(II,III) mixed valence state with respect to disproprotionation. Finally, [**3**][PF_6]$_4$ has a reduction at −1.13 V that is not chemically reversible, while [**4**][PF_6]$_4$ shows two reversible reductions at −0.90 and −1.20 V; based on similar complexes reported these are attributed to the reduction of tpp, since the tpy reductions not visible within the electrochemical window.

Table 1. Electrochemical data for compounds $[1][PF_6]_2$, $[2][PF_6]_2$, $[3][PF_6]_4$ and $[4][PF_6]_4$, recorded in acetonitrile 1.0 M $TBAPF_6$. Peak-to-peak separation (ΔE_p) is shown in brackets. nap = no anodic peak observed and br = broad.

Compound	$E_{½}$ ($V_{Fc/Fc+}$) (ΔE_p (mV))							
	SMe/ SMe^+	Ru'^{II}/ Ru'^{III}	Ru^{II}/ Ru^{III}	tpp/ $tpp^{\cdot-}$	$tpp^{\cdot-}$ /tpp^{2-}	tpy/ $tpy^{\cdot-}$	$tpy^{\cdot-}$ /tpy^{2-}	$\Delta E_{½}$ (ox)
[**1**][PF_6]$_2$	1.08 (nap)		0.87 (83)			-1.62 (95)	-1.92 (100)	
[**2**][PF_6]$_2$	1.22 (nap)		1.06 (93)			-1.49 (179)		
[**3**][PF_6]$_4$	1.88 (204)	1.27 (84)	0.76 (93)	-1.13 (nap)				510
[**4**][PF_6]$_4$	1.93 (155)	1.39 (106)	0.90 (85)	-0.90 (85)	-1.20 (80)			490
[{(tpy)Ru}(μ-tpp){Ru(tpy)}][PF_6]$_4$ [31]		1.35 (85)	1.03 (75)	-0.76 (60)	-1.25 (60)	-1.83 (115)		320

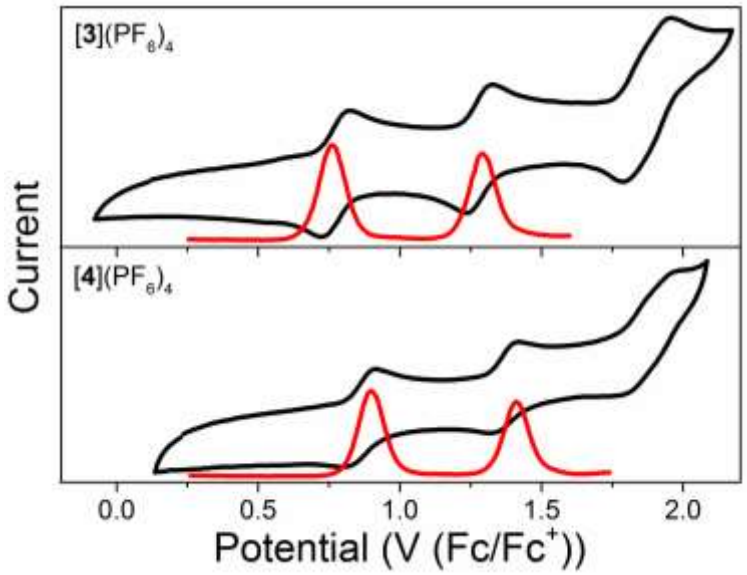

Figure 4. Plots of the CV of [**3**][PF_6]$_4$ and [**4**][PF_6]$_4$, showing the oxidation waves recorded in acetonitrile 1.0 M $TBAPF_6$ at a scan rate of 100 mV s^{-1}.

Based on the onset potentials of the first oxidation and reduction for the compounds [**1**][PF_6]$_2$–[**4**][PF_6]$_4$ the HOMO and LUMO energy levels were determined, using $FeCp_2$ HOMO = −4.8 eV (Table 2).[57] Each of the complexes has a HOMO energy between −5.55 and −5.85 eV, which is relatively close to the work function of clean gold (5.1 - 5.3 eV). The LUMO energy levels are −3.28 to −4.06 eV, which is significantly lower than the work function of clean gold. This could indicate that HOMO type conductance may be favoured for these molecules.

Table 2. HOMO and LUMO energy levels for compounds [1][PF_6]$_2$–[4][PF_6]$_4$ calculated from the onset potentials of the first oxidation and reduction for the compounds.

Compound	HOMO (eV)	LUMO (eV)
[**1**][PF_6]$_2$	-5.67	-3.28
[**2**][PF_6]$_2$	-5.85	-3.46
[**3**][PF_6]$_4$	-5.55	-3.96
[**4**][PF_6]$_4$	-5.68	-4.06

Molecular Conductance.

The single molecule conductance of compounds [**1**][PF_6]$_2$, [**2**][PF_6]$_2$, [**3**][PF_6]$_4$ and [**4**][PF_6]$_4$ was determined using the STM *I*(*s*) method,[36] as described in the experimental section with gold substrates in 1,2,4 – trichlorobenzene solution and electrochemically-etched gold STM tips. A bias voltage of 0.6 V and set point current of 30 nA were employed for [**1**][PF_6]$_2$, [**2**][PF_6]$_2$ and [**3**][PF_6]$_4$ and 10 nA for [**4**][PF_6]$_4$. To record current-distance traces the STM tip was brought close to the Au surface with the applied set point parameters and then the tip was withdraw at a speed of 40 nm/s, and the current-distance (*I*(*s*)) relation was logged. This process

is repeated continuously, and 526, 375, 548 and 290 scans were collected showing characteristic plateaus for [**1**][PF_6]$_2$, [**2**][PF_6]$_2$, [**3**][PF_6]$_4$ and [**4**][PF_6]$_4$ respectively.

The conductance values, 95th percentile break-off distances and calculated molecular lengths are summarised in Table 3, with conductance histograms shown in Figure 5 while representative conductance traces showing current plateaus as well as 2D histograms are given in the supporting information. Note that break-off distances are typically shorter than the length of a fully extended molecular junction. This is consistent with the molecules not being fully extended into a vertical configuration in the gold-molecule-gold junction due to the details of the molecule-surface contact, as well as the stochastic nature of the junction breaking process. In this respect, important points to note about the thiomethyl group are its weaker adsorption to gold than the thiol group and also a degree of steric hindrance provided by the terminal methyl groups which may prevent formation of fully upright configuration for many junction arrangements. It is therefore not surprising that the break-off length fall short of the fully extended junction configuration.

Table 3. Conductance and break-off-distance values for [1][PF_6]$_2$, [2][PF_6]$_2$, [3][PF_6]$_4$ and [4][PF_6]$_4$. Molecular length determined by X-ray analysis and DFT molecular modelling (B3LYP, LANL2DZ/6-31G(d)) are also shown.

Molecule	Conductance (nS)	Measured break off distances and molecular lengths either obtained from X-ray structures or molecular modelling. All distances in nm.		
		Measured 95th Percentile Maximum Break-off distance[a]	X-ray	Molecular model
[**1**][PF_6]$_2$	2.1	1.9	2.15	2.17
[**2**][PF_6]$_2$	1.3	1.8	2.65	2.68
[**3**][PF_6]$_4$	0.78	2.4		2.84
[**4**][PF_6]$_4$	0.43	2.1	3.20	3.35

[a] 95th percentile break-off distance observed across the collected *I*(*s*) scans.

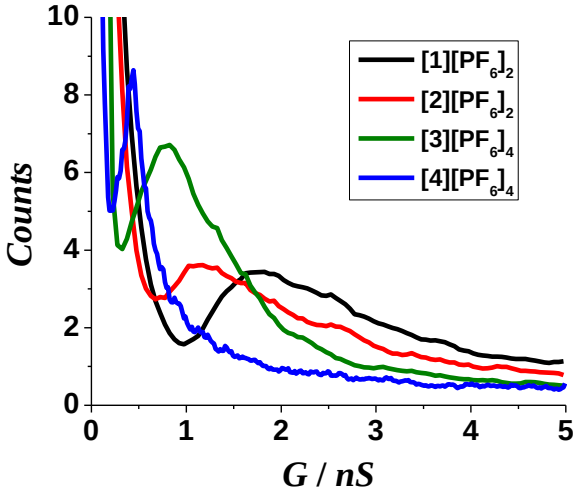

Figure 5. Normalised conductance histograms for the molecular targets.

To appreciate the decay of conductance with molecular length across this series of molecules, Figure 6 plots ln (conductance) versus S…S distance. The conductance is seen to fall off approximately exponentially with molecule length, following the relationship $G \propto e^{\beta L}$, where G is the conductance, L is the length of the molecular bridge and β the tunnelling decay factor. Although the slope of the plot informs about the conductance attenuation with length across this series, it is not strictly a "true β-factor" since this group of molecule does not represent a homologous series in which length is increased by adding repeating moieties (such as methylene groups in an alkanedithiol homologous series). Nevertheless, the length dependence of the conductance is an interesting factor in benchmarking conductance across this series of related molecules. The slope of the ln G versus length plot ("decay factor", β) shown in Figure 6 is 1.5 nm^{-1}. It is instructive to compare this value with other β- values for conjugated aromatic rod-like molecular wires measured in the tunnelling charge transport regime. In the case of oligo(phenylene-ethynylene) molecular wires (OPEs) a β factor of 2.1 nm^{-1} was obtained by Liu et al. with thiol termini,[58] while Kaliginedi *et al*. obtained β = 3.4 nm^{-1}.[5] Lu et al. obtained a β factor of 2.0 nm^{-1} for a series of amine-terminated OPE molecular wires up to 2.75 nm long.[59] Larger decay factors of 4.0 nm^{-1} have been obtained for oligophenylenes. On the other hand smaller decay factors have been recorded for oligo-ynes (0.6 nm^{-1}),[60] oligo-thiophenes (1 nm^{-1}),[61] oligo-porphyrins (0.4 nm^{-1}) and extended viologens (0.06 nm^{-1}).[62, 63] The decay factor across the series of molecules [**1**][PF_6]$_2$ to [**4**][PF_6]$_4$ lies in between decay factors for oligoynes and oligophenylenes, which aligns with our chemical perception of these molecules being less conjugated than the former but more conjugated than the latter. The linear dependence of $\log_e$ (molecular conductance) versus molecular length and the comparative magnitude of the slope points to consistency with a tunnelling mechanism.

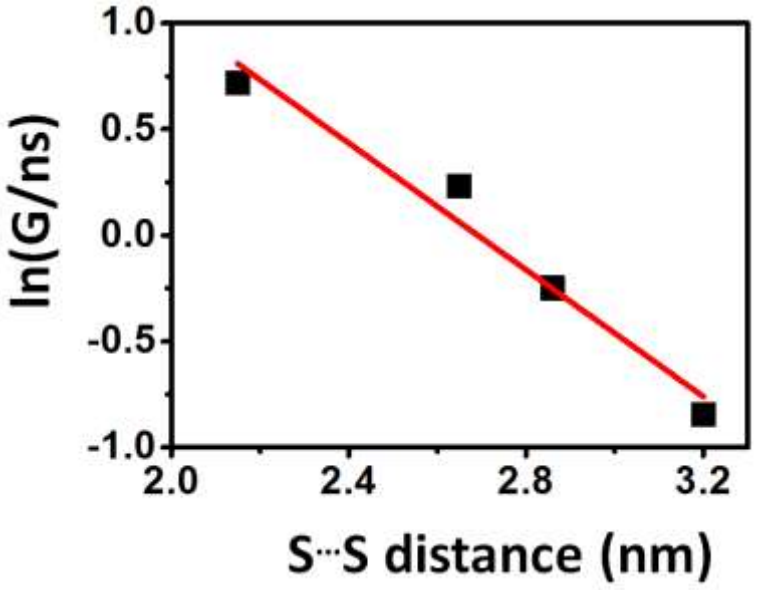

Figure 6. Plot of $\log_e$(G) distance vs. S..S distance (nm).

CONCLUSIONS

The combination of the terpyridine ligands $\mathbf{L}^{\mathbf{1}}$, $\mathbf{L}^{\mathbf{2}}$ and the bridging bis(terchelate) tpp gives the wire-like complexes $[\mathbf{1}]^{2+}$ - $[\mathbf{4}]^{4+}$ with S…S distances spanning up to approximately 3 nm. The pseudo-decay constant extracted from the single molecule conductance values against molecular length is comparable to related organic compounds bearing alkyne and phenylene moieties, with the linear dependence of $\log_e$ (molecular conductance) versus molecular length and the magnitude of the slope consistent with a tunnelling mechanism.

AUTHOR INFORMATION

Corresponding Authors

*Email: paul.low@uwa.edu.au (PJL)

ASSOCIATED CONTENT

Supporting Information. Crystallographic information files (CIF) for compounds $\mathbf{L^2}$, [**2**][PF_6]$_2$·CH_3CN, and [**4**][PF_6]$_4$·3CH_3CN. NMR spectra, selected bond parameters, CV plots and supporting I(s) data.This material is available free of charge via the Internet at http://pubs.acs.org.

ACKNOWLEDGEMENTS

We gratefully acknowledge the EPSRC (EP/K007785/1; EP/K007548/1) for funding this work. P.J.L. gratefully acknowledges support from the Australian Research Council (DP140100855) and the award of a Future Fellowship (FT120100073).

REFERENCES

1. Sun, L.; Diaz-Fernandez, Y. A.; Gschneidtner, T. A.; Westerlund, F.; Lara-Avila, S.; Moth-Poulsen, K., *Chem. Soc. Rev.* **2014,** *43*, 7378-7411.
2. Wang, C. S.; Batsanov, A. S.; Bryce, M. R.; Martin, S.; Nichols, R. J.; Higgins, S. J.; Garcia-Suarez, V. M.; Lambert, C. J., *J. Am. Chem. Soc.* **2009,** *131*, 15647-15654.
3. Moreno-Garcia, P.; Gulcur, M.; Manrique, D. Z.; Pope, T.; Hong, W.; Kaliginedi, V.; Huang, C.; Batsanov, A. S.; Bryce, M. R.; Lambert, C.; Wandlowski, T., *J. Am. Chem. Soc.* **2013,** *135*, 12228-12240.
4. Wold, D. J.; Haag, R.; Rampi, M. A.; Frisbie, C. D., *J. Phys. Chem. B* **2002,** *106*, 2813-2816.

5. Kaliginedi, V.; Moreno-García, P.; Valkenier, H.; Hong, W.; García-Suárez, V. M.; Buiter, P.; Otten, J. L. H.; Hummelen, J. C.; Lambert, C. J.; Wandlowski, T., *J. Am. Chem. Soc.* **2012,** *134*, 5262-5275.

6. Masai, H.; Terao, J.; Seki, S.; Nakashima, S.; Kiguchi, M.; Okoshi, K.; Fujihara, T.; Tsuji, Y., *J. Am. Chem. Soc.* **2014,** *136*, 1742-1745.

7. Lissel, F.; Schwarz, F.; Blacque, O.; Riel, H.; Lörtscher, E.; Venkatesan, K.; Berke, H., *J. Am. Chem. Soc.* **2014,** *136*, 14560-14569.

8. Schwarz, F.; Kastlunger, G.; Lissel, F.; Riel, H.; Venkatesan, K.; Berke, H.; Stadler, R.; Lörtscher, E., *Nano Lett.* **2014,** *14*, 5932-5940.

9. Rigaut, S., *Dalton Trans.* **2013,** *42*, 15859-15863.

10. Low, P. J., *Dalton Trans.* **2005**, 2821-2824.

11. Albrecht, T.; Guckian, A.; Kuznetsov, A. M.; Vos, J. G.; Ulstrup, J., *J. Am. Chem. Soc.* **2006,** *128*, 17132-17138.

12. Albrecht, T.; Moth-Poulsen, K.; Christensen, J. B.; Hjelm, J.; Bjørnholm, T.; Ulstrup, J., *J. Am. Chem. Soc.* **2006,** *128*, 6574-6575.

13. Kastlunger, G.; Stadler, R., *Phys. Rev. B* **2013,** *88*, 035418-035428.

14. Meng, F.; Hervault, Y.-M.; Shao, Q.; Hu, B.; Norel, L.; Rigaut, S.; Chen, X., *Nat Commun* **2014,** *5*, 3023-3032.

15. Osorio, E. A.; Moth-Poulsen, K.; van der Zant, H. S. J.; Paaske, J.; Hedegård, P.; Flensberg, K.; Bendix, J.; Bjørnholm, T., *Nano Lett.* **2009,** *10*, 105-110.

16. Nakamura, H.; Ohto, T.; Ishida, T.; Asai, Y., *J. Am. Chem. Soc.* **2013,** *135*, 16545-16552.

17. Albrecht, T.; Moth-Poulsen, K.; Christensen, J. B.; Guckian, A.; Bjornholm, T.; Vos, J. G.; Ulstrup, J., *Farad. Discuss.* **2006,** *131*, 265-279.

18. Tuccitto, N.; Ferri, V.; Cavazzini, M.; Quici, S.; Zhavnerko, G.; Licciardello, A.; Rampi, M. A., *Nat Mater* **2009,** *8*, 41-46.

19. Wen, H.-M.; Yang, Y.; Zhou, X.-S.; Liu, J.-Y.; Zhang, D.-B.; Chen, Z.-B.; Wang, J.-Y.; Chen, Z.-N.; Tian, Z.-Q., *Chem. Sci.* **2013,** *4*, 2471-2477.

20. Kobayashi, K.; Tonegawa, N.; Fujii, S.; Hikida, J.; Nozoye, H.; Tsutsui, K.; Wada, Y.; Chikira, M.; Haga, M.-a., *Langmuir* **2008,** *24*, 13203-13211.

21. Terada, K.; Kobayashi, K.; Haga, M.-a., *Dalton Trans.* **2008**, 4846-4854.

22. Sakamoto, R.; Katagiri, S.; Maeda, H.; Nishimori, Y.; Miyashita, S.; Nishihara, H., *J. Am. Chem. Soc.* **2015,** *137*, 734-741.

23. Maeda, H.; Sakamoto, R.; Nishihara, H., *Chem.--Eur. J.* **2014,** *20*, 2761-2764.

24. Sakamoto, R.; Ohirabaru, Y.; Matsuoka, R.; Maeda, H.; Katagiri, S.; Nishihara, H., *Chem. Comm.* **2013,** *49*, 7108-7110.

25. Sakamoto, R.; Katagiri, S.; Maeda, H.; Nishihara, H., *Coord. Chem. Rev.* **2013,** *257*, 1493-1506.

26. Ruben, M.; Landa, A.; Lörtscher, E.; Riel, H.; Mayor, M.; Görls, H.; Weber, H. B.; Arnold, A.; Evers, F., *Small* **2008,** *4*, 2229-2235.

27. Ruminski, R. R.; Aasen, T. D., *Inorg. Chim. Acta* **2010,** *363*, 905-910.

28. Padilla, R.; Ruminski, R. R.; Meredith McGinley, V. A.; Williams, P. B., *Polyhedron* **2012,** *33*, 158-165.

29. Yao, C.-J.; Zheng, R.-H.; Nie, H.-J.; Cui, B.-B.; Shi, Q.; Yao, J.; Zhong, Y.-W., *Chem.--Eur. J.* **2013,** *19*, 12376-12387.

30. Yao, C.-J.; Zhong, Y.-W.; Yao, J., *Inorg. Chem.* **2013,** *52*, 4040-4045.

31. Wadman, S. H.; Havenith, R. W. A.; Hartl, F.; Lutz, M.; Spek, A. L.; van Klink, G. P. M.; van Koten, G., *Inorg. Chem.* **2009,** *48*, 5685-5696.

32. Potts, K. T.; Konwar, D., *J. Org. Chem.* **1991,** *56*, 4815-4816.

33. Huang, G.; Yang, C.; Xu, Z.; Wu, H.; Li, J.; Zeller, M.; Hunter, A. D.; Chui, S. S.-Y.; Che, C.-M., *Chem. Mater.* **2009,** *21*, 541-546.

34. Constable, E. C.; Housecroft, C. E.; Medlycott, E.; Neuburger, M.; Reinders, F.; Reymann, S.; Schaffner, S., *Inorg. Chem. Comm.* **2008,** *11*, 518-520.

35. Hartshorn, C. M.; Daire, N.; Tondreau, V.; Loeb, B.; Meyer, T. J.; White, P. S., *Inorg. Chem.* **1999,** *38*, 3200-3206.

36. Haiss, W.; van Zalinge, H.; Higgins, S. J.; Bethell, D.; Höbenreich, H.; Schiffrin, D. J.; Nichols, R. J., *J. Am. Chem. Soc.* **2003,** *125*, 15294-15295.

37. Haiss, W.; Nichols, R. J.; van Zalinge, H.; Higgins, S. J.; Bethell, D.; Schiffrin, D. J., *Phys. Chem. Chem. Phys.* **2004,** *6*, 4330-4337.

38. Sheldrick, G., *Acta Crystallogr., Sect. A* **2008,** *64*, 112-122.

39. Dolomanov, O. V.; Bourhis, L. J.; Gildea, R. J.; Howard, J. A. K.; Puschmann, H., *J. Appl. Crystallogr.* **2009,** *42*, 339-341.

40. M. J. Frisch; G. W. Trucks; H. B. Schlegel; G. E. Scuseria; M. A. Robb; J. R. Cheeseman; G. Scalmani; V. Barone; B. Mennucci; G. A. Petersson; H. Nakatsuji; M. Caricato; X. Li; H. P. Hratchian; A. F. Izmaylov; J. Bloino; G. Zheng; J. L. Sonnenberg; M. Hada; M. Ehara; K. Toyota; R. Fukuda; J. Hasegawa; M. Ishida; T. Nakajima; Y. Honda, O. K., H. Nakai, T. Vreven, J. A. Montgomery, Jr., J. E. Peralta, F. Ogliaro, M. Bearpark, J. J. Heyd, E. Brothers, K. N. Kudin, V. N. Staroverov, R. Kobayashi, J. Normand, K. Raghavachari, A. Rendell, J. C. Burant, S. S. Iyengar, J. Tomasi, M. Cossi, N. Rega, J. M. Millam, M.

Klene, J. E. Knox, J. B. Cross, V. Bakken, C. Adamo, J. Jaramillo, R. Gomperts, R. E. Stratmann, O. Yazyev, A. J. Austin, R. Cammi, C. Pomelli, J. W. Ochterski, R. L. Martin, K. Morokuma, V. G. Zakrzewski, G. A. Voth, P. Salvador, J. J. Dannenberg, S. Dapprich, A. D. Daniels, Ö. Farkas, J. B. Foresman, J. V. Ortiz, J. Cioslowski, and D. J. Fox. *Gaussian 09*, A.1; Gaussian, Inc: Wallingford CT, 2009.

41. Becke, A. D., *The Journal of Chemical Physics* **1993,** *98*, 5648-5652.

42. Stephens, P. J.; Devlin, F. J.; Chabalowski, C. F.; Frisch, M. J., *The Journal of Physical Chemistry* **1994,** *98*, 11623-11627.

43. Hay, P. J.; Wadt, W. R., *The Journal of Chemical Physics* **1985,** *82*, 299-310.

44. Petersson, G. A.; Al-Laham, M. A., *The Journal of Chemical Physics* **1991,** *94*, 6081-6090.

45. Schönherr, H.; Kremer, F. J. B.; Kumar, S.; Rego, J. A.; Wolf, H.; Ringsdorf, H.; Jaschke, M.; Butt, H. J.; Bamberg, E., *J. Am. Chem. Soc.* **1996,** *118*, 13051-13057.

46. Capozzi, B.; Dell, E. J.; Berkelbach, T. C.; Reichman, D. R.; Venkataraman, L.; Campos, L. M., *J. Am. Chem. Soc.* **2014,** *136*, 10486-10492.

47. Wen, H.-M.; Zhang, D.-B.; Zhang, L.-Y.; Shi, L.-X.; Chen, Z.-N., *Eur. J. Inorg. Chem.* **2011,** *2011*, 1784-1791.

48. Du, P.; Schneider, J.; Brennessel, W. W.; Eisenberg, R., *Inorg. Chem.* **2007,** *47*, 69-77.

49. Graczyk, A.; Murphy, F. A.; Nolan, D.; Fernandez-Moreira, V.; Lundin, N. J.; Fitchett, C. M.; Draper, S. M., *Dalton Trans.* **2012,** *41*, 7746-7754.

50. Lee, Y. H.; Nghia, N. V.; Go, M. J.; Lee, J.; Lee, S. U.; Lee, M. H., *Organometallics* **2014,** *33*, 753-762.

51. Maestri, M.; Armaroli, N.; Balzani, V.; Constable, E. C.; Thompson, A. C., *Inorg. Chem.* **1995,** *34*, 2759-2767.

52. Constable, E. C.; Housecroft, C. E.; Medlycott, E.; Neuburger, M.; Reinders, F.; Reymann, S.; Schaffner, S., *Inorg. Chem. Comm.* **2008,** *11*, 518-520.

53. Lashgari, K.; Kritikos, M.; Norrestam, R.; Norrby, T., *Acta Crystallogr., Sect. C: Cryst. Struct. Commun.* **1999,** *55*, 64-67.

54. Yoshikawa, N.; Yamabe, S.; Kanehisa, N.; Inoue, T.; Takashima, H.; Tsukahara, K., *J. Phys. Org. Chem.* **2011,** *24*, 1110-1118.

55. Ghumaan, S.; Sarkar, B.; Chanda, N.; Sieger, M.; Fiedler, J.; Kaim, W.; Lahiri, G. K., *Inorg. Chem.* **2006,** *45*, 7955-7961.

56. Wadman, S. H.; Lutz, M.; Tooke, D. M.; Spek, A. L.; Hartl, F.; Havenith, R. W. A.; van Klink, G. P. M.; van Koten, G., *Inorg. Chem.* **2009,** *48*, 1887-1900.

57. Ahmida, M. M.; Eichhorn, S. H., *ECS Trans.* **2010,** *25*, 1-10.

58. Liu, K.; Li, G.; Wang, X.; Wang, F., *J. Phys. Chem. C* **2008,** *112*, 4342-4349.

59. Lu, Q.; Liu, K.; Zhang, H.; Du, Z.; Wang, X.; Wang, F., *ACS Nano* **2009,** *3*, 3861-3868.

60. Wang, C.; Batsanov, A. S.; Bryce, M. R.; Martín, S.; Nichols, R. J.; Higgins, S. J.; García-Suárez, V. M.; Lambert, C. J., *J. Am. Chem. Soc.* **2009,** *131*, 15647-15654.

61. Yamada, R.; Kumazawa, H.; Noutoshi, T.; Tanaka, S.; Tada, H., *Nano Letters* **2008,** *8*, 1237-1240.

62. Sedghi, G.; Sawada, K.; Esdaile, L. J.; Hoffmann, M.; Anderson, H. L.; Bethell, D.; Haiss, W.; Higgins, S. J.; Nichols, R. J., *J. Am. Chem. Soc.* **2008,** *130*, 8582-8583.

63. Kolivoška, V.; Valášek, M.; Gál, M.; Sokolová, R.; Bulíčková, J.; Pospíšil, L.; Mészáros, G.; Hromadová, M., *J. Phys. Chem. Let.* **2013,** *4*, 589-595.

TABLE OF CONTENTS SYNOPSIS

A series of mono- and bi-metallic ruthenium(II) complexes based on combinations of 2,3,5,6-tetra(pyridine-2-yl)pyrazine and methyl-sulfane substituted 2,2′:6′,2″-terpyridine ligands with lengths of up to 3.2 nm were synthesised. The single molecule conductance behaviour of the series was examined and a pseudo β value for the series determined, lying between those of oligoynes and oligophenylenes.

TABLE OF CONTENTS/ABSTRACTS GRAPHIC